

Re–Os isotope geochemistry in the surface layers of ferromanganese crusts from the Takuyo Daigo Seamount, northwestern Pacific Ocean

AYAKA TOKUMARU,^{1,2,*} TATSUO NOZAKI,^{2,3,4} KATSUHIKO SUZUKI,^{2,3} KOSUKE T. GOTO,^{5,2} QING CHANG,^{2,3} JUN-ICHI KIMURA,² YUTARO TAKAYA,^{6,2} YASUHIRO KATO,^{6,4,3,2} AKIRA USUI^{7,3} and TETSURO URABE¹

¹Department of Earth and Planetary Science, The University of Tokyo, 7-3-1 Hongo, Bunkyo-ku, Tokyo 113-0033, Japan

²Institute for Research on Earth Evolution (IFREE), Japan Agency for Marine–Earth Science and Technology (JAMSTEC), 2-15 Natsushima-cho, Yokosuka, Kanagawa 237-0061, Japan

³Submarine Resources Research Project (SRRP), Japan Agency for Marine–Earth Science and Technology (JAMSTEC), 2-15 Natsushima-cho, Yokosuka, Kanagawa 237-0061, Japan

⁴Department of Systems Innovation, The University of Tokyo, 7-3-1 Hongo, Bunkyo-ku, Tokyo 113-8656, Japan

⁵Geological Survey of Japan (GSJ), National Institute of Advanced Industrial Science and Technology (AIST), Central 7, 1-1-1 Higashi, Tsukuba, Ibaraki 305-8567, Japan

⁶Frontier Research Center for Energy and Resources (FR CER), School of Engineering, The University of Tokyo, 7-3-1 Hongo, Bunkyo-ku, Tokyo 113-8656, Japan

⁷Department of Geology, Natural Sciences Cluster, Kochi University, 2-5-1 Akebono, Kochi 780-8520, Japan

(Received August 13, 2014; Accepted November 26, 2014)

Os isotope compositions in ferromanganese crusts (Fe–Mn crusts) have been used for the dating of model ages from present to the Late Cretaceous. This dating method assumes that the Fe–Mn crusts preserve a paleo-seawater Os isotope composition at the timing of Fe–Mn crust deposition. However, available Os isotope data are limited to dredged samples without precise indications of water depths, and the Os isotope variation in relation to water depth remains uncertain. Here, we report on the Os isotope ratio data in the surface layer of Fe–Mn crusts from 956–2987 meters below sea level at the Takuyo Daigo Seamount in the northwestern Pacific Ocean collected by a remotely operated vehicle (ROV). Since the ¹⁸⁷Re/¹⁸⁸Os ratios of the surface layer samples exhibited low values ranging from 0.020 to 0.0078, the age correction of the ¹⁸⁷Os/¹⁸⁸Os ratios by subtracting radiogenic ¹⁸⁷Os from total ¹⁸⁷Os was not necessary for the Takuyo Daigo Fe–Mn crusts. Regardless of water depth, the surface layer samples possessed a narrow range of ¹⁸⁷Os/¹⁸⁸Os ratio (1.003–1.017). As their Os isotope ratios were very similar to or slightly lower than the present-day seawater value (~1.06), the Fe–Mn crusts are inferred to preserve the modern seawater Os isotope composition at the investigated water depths. Therefore, Os isotope stratigraphy using Fe–Mn crusts is a powerful dating tool in paleoceanography.

Keywords: ferromanganese crust, Re and Os isotopes, geochemistry, Takuyo Daigo Seamount, northwestern Pacific Ocean

INTRODUCTION

Ferromanganese crusts (Fe–Mn crusts) are a type of marine sediment extensively covering the surface of seamounts or oceanic plateaus at depths from 400 to 4000 meters below sea level (mbsl) (Hein *et al.*, 2000). Fe–Mn crusts are typically 1 to 20 cm thick, and their growth rates are 1 to 10 mm/Myr (Hein *et al.*, 2000 and references therein). Fe–Mn crusts concentrate hydrogenous components from ambient seawater and have especially high concentrations of Mn, Co, Ni, Pt and rare earth elements (REEs). Therefore, they are classified as one of the seafloor mineral resources (Hein *et al.*, 2000). More-

over, due to the enrichment of the hydrogenous components and the continuous growth of Fe–Mn crusts, they have been used as a versatile recorder of the seawater chemistry and have been used for paleoceanographic studies (e.g., Christensen *et al.*, 1997; Lee *et al.*, 1999). For younger crusts, absolute dating was attempted using radioactive tracers, such as U–Th (Reyss *et al.*, 1985) and ¹⁰Be/⁹Be (Graham *et al.*, 2004). The ¹⁰Be/⁹Be method is the most widely applied and provides reliable absolute age for crusts younger than 10 Ma (Graham *et al.*, 2004). However, it has been difficult to determine the precise model age of Fe–Mn crusts for older than 10 Ma, and thus a dating method covering the entire age of the deposition of Fe–Mn crusts has long been sought.

Klemm *et al.* (2005) first applied the Os isotope geochronology to Fe–Mn crusts. According to Klemm *et al.* (2005, 2008), the relative age of Fe–Mn crusts can be

*Corresponding author (e-mail: tokumaru@eps.s.u-tokyo.ac.jp)

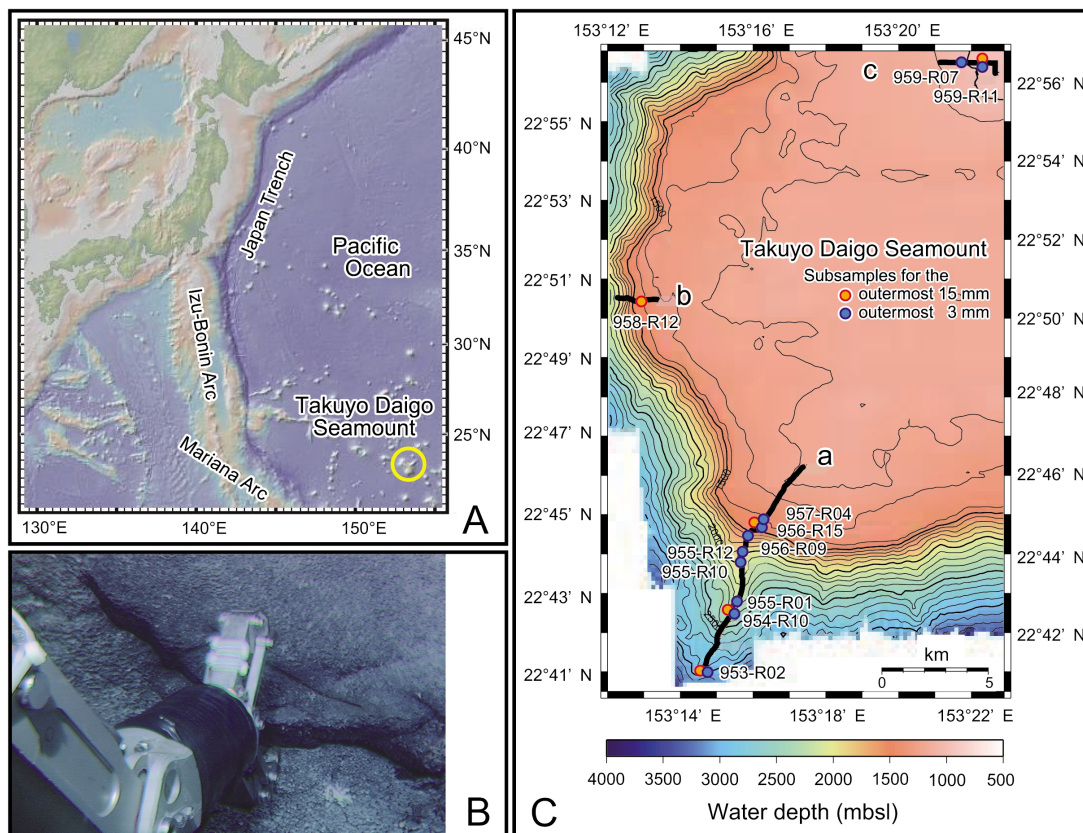


Fig. 1. (A) Index map of the Takuyo Daigo Seamount in the northwestern Pacific Ocean. (B) Sampling photo at 1862 mbsl using a manipulator of ROV Hyper Dolphin 3K (ROV HPD3K). (C) Location map of the samples. The detailed bathymetric map of the southwest side on the Takuyo Daigo seamount was obtained by a multi-narrow beam echo sounder mounted on the RV Natsushima during the NT09-02 cruise. Three diving tracks (a, b and c) of HPD3K are also shown.

determined by comparison between the obtained $^{187}\text{Os}/^{188}\text{Os}$ ratios and the secular variation curve of seawater values reconstructed from marine metalliferous sediments (Peucker-Ehrenbrink and Ravizza, 2012 and references therein). This dating method assumes that Fe–Mn crusts preserve the seawater (hydrogenous) Os isotope composition ($^{187}\text{Os}/^{188}\text{Os}$ ratio) at the time of deposition. The seawater Os isotope composition is balanced by (1) riverine inputs with radiogenic $^{187}\text{Os}/^{188}\text{Os}$ ratios (~ 1.4) and (2) hydrothermal and extraterrestrial inputs with lower $^{187}\text{Os}/^{188}\text{Os}$ ratios (0.12–0.13) into the ocean (Peucker-Ehrenbrink and Ravizza, 2000). The secular variation of seawater Os isotope ratio reflects changes in these fluxes into the ocean. The modern seawater $^{187}\text{Os}/^{188}\text{Os}$ ratio exhibits the highest value of ~ 1.06 during the Cenozoic period due to the increased input of radiogenic Os associated with the Himalayan uplift (Peucker-Ehrenbrink *et al.*, 1995). As the residence time of Os in the ocean is considered to be adequately long compared to the ocean circulation time (10^4 – 10^5 yr; Levasseur, 1998), the concentration and isotope ratio of Os in seawater are glo-

bally homogenous (Levasseur, 1998; Woodhouse *et al.*, 1999).

The Os isotope dating of Fe–Mn crusts, which can be applied from the modern to the Late Cretaceous period, has become more frequently used as a paleoceanographic dating tool (Li *et al.*, 2008; Meng *et al.*, 2008). However, previously obtained Os isotope data are limited to dredged samples, and the Os isotope variation of Fe–Mn crusts in relation to water depth is poorly understood. Using dredged samples of uncertain water depth and surface integrity, Burton *et al.* (1999) reported Os isotope compositions in the surface 0–0.5 mm layer of Fe–Mn crusts from various ocean basins and found that most of the Os isotope compositions are very similar to those of modern seawater. However, some samples exhibit a remarkably unradiogenic $^{187}\text{Os}/^{188}\text{Os}$ ratio of ~ 0.5229 due to the direct incorporation of micrometeoritic or abyssal peridotite particles (Burton *et al.*, 1999). Moreover, the concentrations and isotope compositions of Os in the surface 0–0.5 mm layer show some variations even within a single seamount.

Table 1. Sample list of the Takuyo Daigo Fe–Mn crusts used for Re and Os isotope analyses

Sample No.	Dive track ^b	Water depth (mbsl)	Thickness of Fe–Mn oxide layer ^c (mm)	The surface 0–15 mm layer	The surface 0–3 mm layer
HPD#959-R11	c	965	1.2–23.0	○	○
HPD#959-R07	c	1019	3.9–46.6	—	○
HPD#957-R04-A ^a	a	1418	15.9–39.3	—	○
HPD#957-R04-B ^a	a	1418			○
HPD#958-R12	b	1424	18.3–34.0	○	○
HPD#956-R15-A ^a	a	1440	11.1–65.3	○	○
HPD#956-R15-B ^a	a	1440		○	
HPD#956-R09	a	1626	5.9–18.2	—	○
HPD#955-R12	a	1937	9.1–34.5	—	○
HPD#955-R10-A ^a	a	2008	10.0–45.3	—	○
HPD#955-R10-B ^a	a	2008			○
HPD#955-R01-A ^a	a	2209	32.1–50.0	—	○
HPD#955-R01-B ^a	a	2209			○
HPD#954-R10	a	2239	30.3–35.7	○	○
HPD#953-R02	a	2987	9.7–19.4	○	○

^aPowder samples were prepared from different parts of the surface layer from the same rock sample.

^bSee Fig. 1C for each dive track and sample locality.

^cFe–Mn oxide shows the black layered section that covers the bedrock, which can be easily distinguished from its appearance. Thicknesses were measured based on the rock samples employed for the surface 0–3 mm layer analysis.

As the surface 0–0.5 mm layer might be susceptible to particle incorporation, we analyzed the concentrations and isotope ratio data of Re and Os in the surface 0–3 mm and 0–15 mm layers of Fe–Mn crusts, which were collected from various water depths of the Takuyo Daigo Seamount in the northwestern Pacific Ocean. Sampling was improved by using the remotely operated vehicle *Hyper Dolphin 3K* (ROV HPD3K) to avoid any disturbance of the Fe–Mn crusts.

MATERIALS AND METHODS

Sampling site and methods

The Takuyo Daigo Seamount is located about 150 km southwest of the Minamitorishima Island in the northwestern Pacific Ocean (23°00' N, 153°20' E, Fig. 1A). The ⁴⁰Ar/³⁹Ar age of the seamount basalt was 100.4 ± 2.3 Ma (Tokumaru *et al.*, unpubl. data), which is consistent with the ages of other seamounts distributed in the Wake Seamount Trail (Koppers *et al.*, 2003). The Fe–Mn crust samples were collected during the NT09-02 Leg. 2 cruise from 8 February 2009 to 24 February 2009 by the *RV Natsushima* equipped with a ROV HPD3K. This was the first research cruise that was dedicated only for investigating Fe–Mn crusts. For the crust sampling, the manipulator of the HPD3K was used with an underwater diamond saw and a pinch bar while outcrop features were observed (Fig. 1B). Seven dives were carried out at the Takuyo Daigo Seamount, and 108 samples in total were systematically collected within a depth range from 947

to 2991 mbsl (Fig. 1C).

The Fe–Mn crust samples were washed with tap water and kept in sealed plastic bags on board the *RV Natsushima* at room temperature. Block samples were cut into several slabs (width 2–3 cm) perpendicular to the growth layer. For the Re and Os isotope analyses, Fe–Mn crust samples with intact and undisturbed surfaces were selected (Supplementary Fig. S1 and Table 1). Each surface layer was sliced to a thickness range of 0–3 mm or 0–15 mm by a diamond cutter, with care not to include obviously altered or incorporated section (Fig. S1). As the surface 0–0.5 mm layer might be susceptible to particle incorporation, we analyzed the concentrations and isotope ratios of Re and Os in the surface 0–3 mm and 0–15 mm layers of Fe–Mn crusts, which were collected from various water depths of the Takuyo Daigo Seamount in the northwestern Pacific Ocean. These outermost 3-mm and 15-mm layer samples are expected to be more homogeneous than the 0.5-mm layer samples from Burton *et al.* (1999). Several outermost 15-mm layer samples were preliminarily made for their precise Re/Os ratio and Re content measurement. In order to understand the spatial heterogeneity of Re and Os isotope ratio data within one sample, duplicate slices of the surface layer were prepared to provide several subsamples (Table 1). The sliced samples were carefully polished by a diamond plate to avoid any contamination from the diamond cutter. After a rinsing with de-ionized Milli-Q water, the samples were pulverized in an agate mortar.

Chemical analysis

All Re–Os isotope analyses were carried out at Institute for Research on Earth Evolution (IFREE), Japan Agency for Marine–Earth Science and Technology (JAMSTEC). The concentrations and isotope ratios of Re and Os were determined by isotope dilution multi-collector inductively coupled plasma mass spectrometry (ID-MC-ICP-MS) combined with a Carius tube digestion, sparging Os introduction and Re separation by anion exchange chromatography (Morgan *et al.*, 1991; Shirey and Walker, 1995; Hassler *et al.*, 2000; Schoenberg *et al.*, 2000). This combination of the sparging introduction method with MC-ICP-MS was developed for simple and rapid determination of Re–Os isotopes (Nozaki *et al.*, 2012). The sparging introduction is a technique in which volatile OsO_4 molecules go directly into the ICP glass torch, along with exchange of the introduction tubing connected to the ICP glass torch for each sample. Ar carrier gas was bubbled into the sample solution in a Teflon sample vial through a Teflon transfer cap with 1/8-inch Teflon tubings at room temperature (Hassler *et al.*, 2000). In order to avoid any droplets from the sample vial, another Teflon vial was placed between the sample vial and the ICP glass torch (Norman *et al.*, 2002). Schematic diagram of the sample introduction system is shown in Supplementary Fig. S2, and detailed analytical protocols including measured data corrections and error calculations are given in Nozaki *et al.* (2012). In comparison with an analytical procedure by using a thermal ionization mass spectrometry in negative ion mode (N-TIMS), the Os blanks for the sparging method were lowered due to the simplification of the sample preparations and the reduction of the amounts and kinds of reagents. In addition, the Os memory effect does not alter the result, as the carryover of Os quickly decreased to several tens of counts per second on ^{188}Os by flowing Ar gas into the introduction tubing for ca. 10 seconds as well as the exchange to the new Teflon transfer cap with 1/8-inch Teflon tubings. Thus, it is suitable for measuring low Os concentrations or small sample amounts. The measured data were corrected by means of the standard bracketing method in order to correct the yields of the multi ion-counters that change with time.

The powdered samples (~50 mg for the surface 0–3 mm layer samples and ~200 mg for the surface 0–15 mm layer samples) were digested and equilibrated with ^{185}Re and ^{190}Os spike solutions in 4 mL inverse *aqua regia* ($\text{HCl}:\text{HNO}_3 = 1:3$) at 220°C for 24 h in a Carius tube. The Carius tubes were opened carefully, and the sample solutions were transferred to 30 mL Teflon vials containing 13 mL of de-ionized Milli-Q water. The Os isotope ratios were determined by MC-ICP-MS (Thermo Fisher Scientific NEPTUNE) with the sparging introduction of OsO_4 molecules to the ICP glass torch. After the Os meas-

urement, the sample solutions were heated on a hotplate at 140 °C to remove any remaining Os. Re was then separated from the aqueous phase by means of Muromac AG 1-X8 anion exchange resin. The Re isotope ratios were also measured by NEPTUNE with a desolvent nebulizer (Aridus II; CETAC Technologies). All obtained data were corrected for procedural Re and Os blank values of 6.38 and 0.70–1.01 pg with a $^{187}\text{Os}/^{188}\text{Os}$ ratio of ~0.15, respectively.

The operating conditions for MC-ICP-MS measurements were tuned to achieve the maximum ion intensities for ^{188}Os and ^{187}Re using the oxidized JMC Os standard solution containing 50 pg of total Os and a 10 pg/g in-house Re standard solution, respectively. Details of the operating conditions are given in Supplementary Material (Supplementary Table S1). Mass fractionations within NEPTUNE and the change of yields among four ion-counters with time were corrected by the standard bracketing method. The Os isotope ratios were calculated based on the summation of the ion intensities during one measurement (30 cycles), as the detected Os isotope ratio drifts during measurement by the change of yields of the multi ion-counters with time. The precision of the Os isotope ratios was determined based on the additivity of variance by using the variance in the ion intensity of each Os isotope. As the first and last samples within one analytical batch, we additionally measured the Os ion intensities of the Ar gas blank, and average Os ion intensities of these two Ar gas blanks were subtracted from those of other samples. This is an additional analytical improvement from the method of Nozaki *et al.* (2012) and ^{185}Re ion intensity was at most several counts per second which was negligible for the sample measurements. The Re isotope ratio was calculated as an average value within one measurement (30 cycles), as the ion intensity and the isotope ratio were stable during the measurement because the Re isotopes were measured with solution nebulization and detected by Faraday cups. The variance in the Re isotope ratio was simply determined using thirty measured values. Finally, precisions in the Os and Re isotope ratios were calculated on the basis of the error propagation using the variances through the isotope dilution method. During the Re isotope measurements, the ion intensity of ^{192}Os was also monitored for isobaric interference correction on mass 187, however, we could not detect any ^{192}Os ion intensities by Faraday cups, then no isobaric interference corrections on mass 187 was conducted. Detailed analytical procedures and correction methods are given in Nozaki *et al.* (2012).

Major element analyses for the outermost 15-mm layer samples were obtained by Fusion Inductively Coupled Plasma (FUS-ICP) at Activation Laboratories in Canada according to Code 4B analytical package. The powdered sample was progressively dried at 110°C and sent to Ac-

Table 2. Re and Os geochemical compositions in the surface 0–15 mm layer of Fe–Mn crusts from the Takuyo Daigo Seamount

Sample No.	Water depth (mbsl)	Re (ppt)	ISD	Os (ppt)	ISD	$^{187}\text{Re}/^{188}\text{Os}$	ISD	$^{187}\text{Os}/^{188}\text{Os}$	ISD
HPD#959-R11	965	6.963	0.026	1508	9	0.02463	0.00018	0.949	0.005
HPD#958-R12	1424	18.25	0.04	1243	7	0.0777	0.0005	0.875	0.005
HPD#956-R15-A*	1440	9.461	0.022	1296	13	0.0392	0.0004	1.006	0.008
HPD#956-R15-B*	1440	5.394	0.018	1483	12	0.01952	0.00017	1.002	0.006
HPD#954-R10	2239	12.75	0.04	1753	26	0.0393	0.0006	1.071	0.011
HPD#953-R02	2987	14.79	0.05	1613	20	0.0493	0.0006	1.014	0.008

All data are blank corrected and errors are ISD. The variance in the ion intensity of each Os isotope was determined using sixty data obtained for ^{187}Os and ^{188}Os or thirty data obtained for ^{190}Os and ^{192}Os , assuming that ion intensity decay was described by the Poisson distribution. The variance in the Os isotope ratio can be calculated based on additivity of variance. The variance in the Re isotope ratio was simply determined using thirty measured values, as the ion intensity and the isotope ratio were stable during the measurement. Finally, precisions in our Re–Os data were calculated on the basis of the error propagation using these variances through the isotope dilution method (Nozaki *et al.*, 2012).

*Powder samples were prepared from different parts of the surface layer from the same rock sample.

tivation Laboratories for the analysis. In order to digest powder sample completely, sample powders were mixed with lithium metaborate/tetraborate followed by fusion in an induction furnace. The molten melts were dissolved in the nitric acid solutions, which were diluted before introduction into the ICP-OES (Thermo Jarrell-Ash ENVIRO II ICP or Varian Vista 735 ICP).

Major element concentrations of the outermost 3-mm layer samples were determined by ICP mass spectrometry (ICP-MS; Agilent 7500c) at Department of Systems Innovations, the University of Tokyo. Powdered splits (~50 mg) were dissolved by HNO_3 – HF – HClO_4 digestion in tightly sealed Teflon PFA screw-cap beakers, heated for 12 hours on a hot plate at 130°C. The decomposed sample was progressively evaporated at 110°C for 12 hours, 160°C for 6 hours, and 190°C for 3 hours until dryness. Subsequently, 4 mL HNO_3 , 1 mL HCl and 5 mL de-ionized Milli-Q was added to the residue, and the solution was diluted to 1:8000 by mass. The ICP-MS analytical procedures we used have been fully described in Kato *et al.* (2011).

Electron microscopic characterizations

The block sample was cut into a slab (width 2–3 cm) perpendicular to the growth layer. The slab was embedded in an epoxy resin to avoid disruption, before sliced and polished into the thin section (Fig. S2A). The polished surface of the thin section was coated with carbon and characterized by scanning electron microscope (SEM; Hitachi S4500) coupled to energy dispersive X-ray (EDX) microanalysis operated at 15-kV accelerating voltage.

RESULTS AND DISCUSSION

Outcrop features of Fe–Mn crusts

The summit of the Takuyo Daigo Seamount (950 mbsl) was covered by thick consolidated lagoon sediments with

milky carbonate matrix. On the other hand, steep slopes or escarpments around the flat top at 1500–2990 mbsl were composed of pillow basalts, sheet flows, pyroclastic rocks, gravels and talus deposits. Fe–Mn crusts were observed at all outcrops between 950 and 2990 mbsl. The summit area was covered by thin Fe–Mn crusts in place, whereas thick Fe–Mn crusts were distributed around slopes or escarpments at 1500–2500 mbsl. The thicknesses of the 108 Fe–Mn crust samples showed a range from <1 to 100 mm with no clear correlation with water depth, and the average thickness was 34.5 mm (Table 1).

Os and Re vertical profiles of the outermost 15-mm layer

Re and Os concentrations in the surface 0–15 mm layer were 5.394–18.25 ppt and 1243–1753 ppt, respectively (Table 2). The Re and Os concentrations showed no systematic variations with water depth (Figs. 2A and C). $^{187}\text{Os}/^{188}\text{Os}$ ratio in the surface 0–15 mm layer was from 0.875 to 1.071 (Table 2). The $^{187}\text{Os}/^{188}\text{Os}$ ratio also showed no systematic variations with respect to water depth (Fig. 2B). The $^{187}\text{Os}/^{188}\text{Os}$ ratios of two powder samples prepared from the same Fe–Mn crust sample (HPD#956-R15-A and -B) were identical within their errors.

The $^{187}\text{Os}/^{188}\text{Os}$ ratio of HPD#958-R12 (0.875) was significantly lower than those of the other samples. The MgO concentration in HPD#958-R12 (1424 mbsl) was slightly higher compared to that of HPD#956-R15 (1440 mbsl) (Table 3), although the sampled water depths were close to each other. We found small Mg-rich silicate particles of (<0.3 mm in size) using SEM coupled to EDX microanalysis that was not detected by transmitted light microscopic observation (Supplementary Fig. S3). The particle was also enriched with potassium, calcium, sodium and iron. As aluminum was not detectable in the EDX spectra, the Mg-rich silicate particles might be the alteration product of basaltic rocks such as saponite (Alt

Table 3. Major compositions in the surface 0–15 mm layer of Fe–Mn crusts from the Takuyo Daigo Seamount

Sample No.	Water depth (mbsl)	SiO ₂ (%)	Al ₂ O ₃ (%)	Fe ₂ O ₃ * (%)	MnO (%)	MgO (%)	CaO (%)	Na ₂ O (%)	K ₂ O (%)	TiO ₂ (%)	P ₂ O ₅ (%)
Detection limit		0.01	0.01	0.01	0.001	0.01	0.01	0.01	0.01	0.001	0.01
HPD#959-R11	965	2.97	0.82	16.84	29.73	1.58	2.68	1.07	0.44	0.87	0.83
HPD#958-R12	1424	8.28	1.83	18.19	25.14	1.48	2.80	1.31	0.51	1.09	1.03
HPD#956-R15	1440	9.67	1.50	20.66	24.51	1.33	2.52	1.34	0.48	1.10	0.93
HPD#954-R10	2239	9.32	1.48	21.75	22.57	1.30	2.40	1.22	0.50	1.18	0.80
HPD#953-R02	2987	6.59	1.01	22.54	23.38	1.29	2.36	1.10	0.41	1.39	0.73

Fe₂O₃*: Total iron is expressed as Fe₂O₃.

et al., 1992). Because seamount basaltic rocks show unradiogenic ¹⁸⁷Os/¹⁸⁸Os ratio of 0.12–0.13 (Peucker-Ehrenbrink and Ravizza, 2000), the low ¹⁸⁷Os/¹⁸⁸Os ratio in HPD#958-R12 was most likely due to the incorporation of altered seamount basaltic fragments into the surface layer. The mixing fraction of Os derived from seamount basaltic fragments was calculated to be 19.9% using a simple mass balance equation based on Os isotope ratios, assuming that the ¹⁸⁷Os/¹⁸⁸Os ratio of seawater is 1.06 (Peucker-Ehrenbrink *et al.*, 1995) and ¹⁸⁷Os/¹⁸⁸Os ratio of basalt is 0.1314 (Gannoun *et al.*, 2007). It should be noted that this mixing fraction (19.9%) is the maximum estimate because the seawater Os isotope ratio rapidly increased from the Oligocene to present associated with the Himalayan uplift (Peucker-Ehrenbrink *et al.*, 1995) and 15 mm thickness of Fe–Mn crust has average chemical information during several Myr based on the common growth rate (1 to 10 mm/Myr).

In order to determine the initial ¹⁸⁷Os/¹⁸⁸Os ratio to reconstruct the paleo-seawater Os isotope ratio from the sedimentary rocks, it is necessary to subtract the radiogenic ¹⁸⁷Os from the total ¹⁸⁷Os (age correction of internal decay). The initial ¹⁸⁷Os/¹⁸⁸Os ratio can be calculated by the following equation:

$$\left(\frac{^{187}\text{Os}}{^{188}\text{Os}}\right)_i = \left(\frac{^{187}\text{Os}}{^{188}\text{Os}}\right)_t - \left(\frac{^{187}\text{Re}}{^{188}\text{Os}}\right) \left(e^{\lambda t} - 1\right)$$

where (¹⁸⁷Os/¹⁸⁸Os)_t and (¹⁸⁷Os/¹⁸⁸Os)_i denote present and initial ¹⁸⁷Os/¹⁸⁸Os ratios, λ denotes the decay constant of ¹⁸⁷Re (1.666 × 10⁻¹¹; Smoliar *et al.*, 1996), and t denotes the sedimentary age of a rock sample. The ¹⁸⁷Re/¹⁸⁸Os ratios of the Takuyo Daigo Fe–Mn crusts ranged from 0.020 to 0.078 (Fig. 2D and Table 2), which is much lower than those of black shales and other sedimentary rocks (Peucker-Ehrenbrink and Ravizza, 2000). Even if we assume a sedimentary age of 100 Ma (t = 100 × 10⁶ yr) and a maximum ¹⁸⁷Re/¹⁸⁸Os ratio of ~0.078, the differences between initial and present ¹⁸⁷Os/¹⁸⁸Os ratios were less than 0.0002. As the difference is smaller than the analyti-

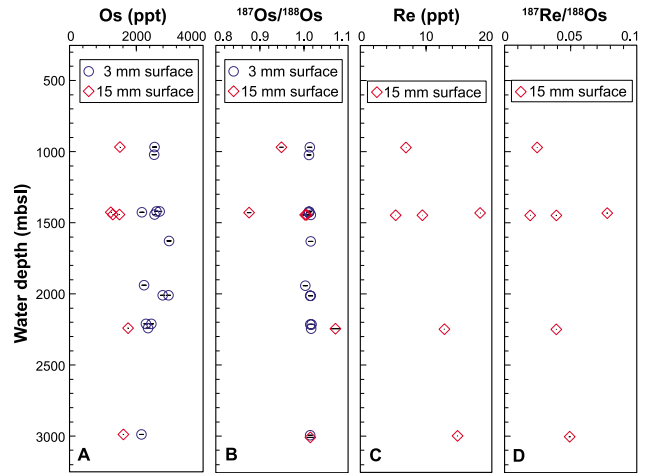


Fig. 2. Water depth variations of (A) Os content, (B) ¹⁸⁷Os/¹⁸⁸Os ratio, (C) Re content and (D) ¹⁸⁷Re/¹⁸⁸Os ratio of the Fe–Mn crust surface layers from the Takuyo Daigo Seamount. Blue and red symbols indicate the surface 0–3 mm and 0–15 mm layers, respectively. All errors expressed as 1SD (standard deviation) are shown as black bars and are smaller than the symbols. The lower ¹⁸⁷Os/¹⁸⁸Os ratio in the sample HPD#958-R12 (1424 mbsl) was possibly due to the incorporation of altered seamount basaltic fragments into the surface layer.

cal errors (1 SD) of measured ¹⁸⁷Os/¹⁸⁸Os ratios, the age correction was not conducted (Tables 2 and 4).

Os vertical profile from the outermost 3-mm layer

The Os concentrations in the surface 0–3 mm layer at 11 different water depths ranged from 2154 to 2980 ppt (Fig. 2A and Table 4) with no systematic variations with water depth. The ¹⁸⁷Os/¹⁸⁸Os ratios in the surface 0–3 mm layer exhibited fairly homogenous values from 1.003 to 1.017 (Fig. 2B and Table 4). Three sets of subsamples duplicated from the same Fe–Mn crust samples (HPD#957-R04, HPD#955-R10 and HPD#955-R01) showed slight variations of Os concentration within 10% (Fig. 2A and Table 4), whereas the ¹⁸⁷Os/¹⁸⁸Os ratios of these subsamples were identical within analytical errors.

Table 4. Os concentration and isotope ratio for the surface 0–3 mm surface layer of Fe–Mn crusts from the Takuyo Daigo Seamount

Sample No.	Water depth (mbsl)	Os (ppt)	1SD	$^{187}\text{Os}/^{188}\text{Os}$	1SD
HPD#959-R11	965	2546	15	1.013	0.005
HPD#959-R07	1019	2535	16	1.011	0.005
HPD#957-R04-A*	1418	2167	13	1.010	0.005
HPD#957-R04-B*	1418	2699	16	1.012	0.005
HPD#958-R12	1424	2603	16	1.011	0.005
HPD#956-R15	1440	2546	15	1.015	0.005
HPD#956-R09	1626	2980	18	1.015	0.005
HPD#955-R12	1937	2232	12	1.003	0.005
HPD#955-R10-A*	2008	2964	16	1.015	0.004
HPD#955-R10-B*	2008	2789	16	1.014	0.005
HPD#955-R01-A*	2209	2288	12	1.014	0.005
HPD#955-R01-B*	2209	2450	19	1.017	0.007
HPD#954-R10	2239	2351	11	1.016	0.004
HPD#953-R02	2987	2154	11	1.014	0.004

All data are blank corrected and errors are 1SD. The variance in the ion intensity of each Os isotope was determined using sixty data obtained for ^{187}Os and ^{188}Os or thirty data obtained for ^{190}Os and ^{192}Os , assuming that ion intensity decay was described by the Poisson distribution. The variance in the Os isotope ratio can be calculated based on additivity of variance. Finally, precisions in our Re–Os data were calculated on the basis of the error propagation using these variances through the isotope dilution method (Nozaki *et al.*, 2012).

*Powder samples were prepared from different parts of the surface layer from the same rock sample.

Table 5. Major compositions in the surface 0–3 mm surface layer of Fe–Mn crusts from the Takuyo Daigo Seamount

Sample No.	Water depth (mbsl)	Al (%)	Fe (%)	Mn (%)	Mg (%)	Ca (%)	Na (%)	K (%)	Ti (%)	P (%)
HPD#959-R11	965	0.30	13.24	23.21	1.04	1.96	0.92	0.31	0.62	0.47
HPD#959-R07	1019	0.33	13.02	24.55	1.10	1.98	1.19	0.36	0.67	0.46
HPD#957-R04-A*	1418	0.61	15.07	21.20	1.01	1.90	0.84	0.38	0.71	0.46
HPD#957-R04-B*	1418	0.49	13.53	21.64	0.99	1.86	0.88	0.37	0.62	0.44
HPD#958-R12	1424	0.91	15.31	19.10	1.01	1.71	0.93	0.39	0.65	0.47
HPD#956-R15	1440	0.59	15.04	20.04	0.96	1.86	1.04	0.38	0.69	0.48
HPD#956-R09	1626	0.74	15.00	19.50	0.96	1.77	0.93	0.43	0.79	0.41
HPD#955-R12	1937	0.85	17.92	18.63	0.97	1.87	0.99	0.46	0.77	0.44
HPD#955-R10-A*	2008	0.80	14.48	19.08	0.97	1.89	0.91	0.45	0.73	0.38
HPD#955-R10-B*	2008	0.94	15.60	19.03	1.00	1.85	0.86	0.46	0.77	0.40
HPD#955-R01-A*	2209	0.97	16.50	18.14	0.99	1.91	1.08	0.48	0.74	0.41
HPD#955-R01-B*	2209	0.68	16.62	19.48	1.00	1.90	1.10	0.44	0.77	0.40
HPD#954-R10	2239	0.64	16.88	19.31	0.97	1.90	0.99	0.42	0.73	0.44
HPD#953-R02	2987	0.91	18.23	16.82	0.94	1.67	1.04	0.46	0.84	0.40

*Powder samples were prepared from different parts of the surface layer from the same rock sample.

The $^{187}\text{Os}/^{188}\text{Os}$ ratios from various water depths showed close agreement within ± 1 SD, except for the slightly low ratio (~ 1.003) of HPD#955-R12. As the $^{187}\text{Os}/^{188}\text{Os}$ ratio in the global seawater increases rapidly during the Quaternary (Peucker-Ehrenbrink *et al.*, 1995), the $^{187}\text{Os}/^{188}\text{Os}$ ratios in the surface layer of Fe–Mn crusts may reflect even small differences of growth rate. Thus, it is noteworthy that all $^{187}\text{Os}/^{188}\text{Os}$ ratios in the surface 0–3 mm layers were consistent within ± 2 SD. Alternatively, the incorporation of altered seamount basaltic rocks with unradiogenic $^{187}\text{Os}/^{188}\text{Os}$ ratios may explain the observed low $^{187}\text{Os}/^{188}\text{Os}$ ratio. However, this was not evident from major composition analysis (Table 5) and SEM-EDX

analysis. Although we cannot rule out the possibility of the presence of undetectable Mg-rich silicate particles, the observed low $^{187}\text{Os}/^{188}\text{Os}$ ratio likely reflects the relatively slow growth rate of HPD#955-R12.

Validity of Os isotope geochronology

Os is classified as a conservative element whose concentration is constant regardless of water depth in seawater (Levasseur, 1998; Woodhouse *et al.*, 1999). The relatively narrow range of Os concentration and the absence of any systematic correlation with water depth obtained in the present study is consistent with the depth profile of Os concentration in the Pacific Ocean

(Woodhouse *et al.*, 1999).

The average Os concentration in the surface 0–3 mm layer was 2522 ppt, which was higher than that in the surface 0–15 mm layer (1483 ppt) (Tables 2 and 3). The Os concentrations of Fe–Mn crusts reported in the previous studies have shown a continuous decrease from the surface to the inner part (Klemm *et al.*, 2005, 2008). Moreover, the seawater $^{187}\text{Os}/^{188}\text{Os}$ ratio tends to increase from the Oligocene to the present, which is interpreted as resulting from the increased input of radiogenic Os by the Himalayan uplift (e.g., Pegram *et al.*, 1992; Ravizza, 1993; Peucker-Ehrenbrick *et al.*, 1995; Pegram and Turekian, 1999). It is therefore plausible that the average Os concentration and the average $^{187}\text{Os}/^{188}\text{Os}$ ratio in the surface 0–3 mm layer were higher than those in the surface 0–15 mm layer reflecting the secular changes of the global seawater.

The $^{187}\text{Os}/^{188}\text{Os}$ ratios in the surface 0–3 mm layer displayed a narrow range (Fig. 2B). Modern seawater $^{187}\text{Os}/^{188}\text{Os}$ ratios have been directly measured to be globally homogeneous in the water columns of the Eastern Pacific and the Indian Ocean (Levasseur, 1998; Woodhouse *et al.*, 1999). The very small variation of $^{187}\text{Os}/^{188}\text{Os}$ ratio with water depth indicates that the sedimentary age of the surface 0–3 mm layer is almost the same for all the water depths (Fig. 2B). This conclusion is consistent with the $\delta^{234}\text{U}$ data obtained from the same powdered samples ($\delta^{234}\text{U} = 102\text{--}135\%$; Goto *et al.*, 2014), which suggest that surface 0–3 mm layers were formed in the limited period of modern seawater (30–129 kyr). In addition, the surface 0–3 mm layer of Fe–Mn crusts from the Magellan Seamount sample, near the Takuyo Daigo Seamount has been dated to be 0.3 Ma by Usui *et al.* (2007) on the basis of $^{10}\text{Be}/^9\text{Be}$ dating. They also analyzed five samples from seamounts on the Philippine Sea Plate and found that the extrapolated surface ages from $^{10}\text{Be}/^9\text{Be}$ curves are zero within the analytical error. These results also support our conclusion that the surface ages of Fe–Mn crusts are close to zero in the north-western Pacific Ocean. The average $^{187}\text{Os}/^{188}\text{Os}$ ratio (1.013) in the surface 0–3 mm layer was slightly lower than that of the modern seawater value (~ 1.06) (Levasseur, 1998; Woodhouse *et al.*, 1999). The low average value indicates that the surface 0–3 mm layer includes portions with lower $^{187}\text{Os}/^{188}\text{Os}$ values compared to that of modern seawater. Although the possibility of the regional variation in seawater $^{187}\text{Os}/^{188}\text{Os}$ ratio (Paquay and Ravizza, 2012) cannot be ruled out, these lower $^{187}\text{Os}/^{188}\text{Os}$ values are more likely due to the rapid increase of the $^{187}\text{Os}/^{188}\text{Os}$ ratio in the global seawater throughout the Quaternary (e.g., Pegram *et al.*, 1992; Ravizza, 1993; Peucker-Ehrenbrick *et al.*, 1995; Pegram and Turekian, 1999). These geochemical lines of evidence indicate that Fe–Mn crusts preserve the Os isotope composition of ambient

seawater, which strongly supports the view that Os isotope geochronology is a reliable tool for dating a broad age ranging from the Late Cretaceous to the modern era.

CONCLUSIONS

As the $^{187}\text{Re}/^{188}\text{Os}$ ratios in the surface 0–15 mm layer had much smaller values (0.020–0.078) than those of other sedimentary rocks, the age correction for ^{187}Re internal decay was found to be negligible for determining the initial $^{187}\text{Os}/^{188}\text{Os}$ ratios. The $^{187}\text{Os}/^{188}\text{Os}$ ratios in the surface 0–3 mm layer of Fe–Mn crusts obtained from the Takuyo Daigo Seamount showed quite homogeneous values from 1.003 to 1.017 regardless of water depth (956–2987 mbsl). The $^{187}\text{Os}/^{188}\text{Os}$ ratios of the Fe–Mn crusts were very similar to or slightly lower than that of the present-day ambient seawater (~ 1.06), reflecting the secular changes of the global seawater. Taken all together, Os isotope chronology on Fe–Mn crusts is thus a powerful tool for paleoceanographic study.

Acknowledgments—We thank R. Senda, H. Yamamoto and Y. Otsuki for assistance with the Re and Os isotope analyses. We also wish to thank the captain and crew of the *RV Natsushima* and the operation team of the *Hyper Dolphin 3K* for their technical expertise. We acknowledge K. Ichimura for his technical support during SEM-EDX microanalysis. Early versions of this manuscript were much improved by comments from Y. Suzuki and the proofreading/editing assistance from the GCOE program. This study was supported by “TAIGA” project as a Scientific Research on Innovative Areas by grants-in-aid for scientific research from the Japanese Ministry of Education, Culture, Sports, Science and Technology (MEXT).

REFERENCES

- Alt, J. C., France-Lanord, C., Floyd, P., Castillo, P. and Galy, A. (1992) Low-temperature hydrothermal alteration of Jurassic ocean crust, Site 801. *Proc. ODP Sci. Res.* **129**, 415–427.
- Burton, K. W., Bourdon, B., Birck, J.-L., Allègre, C. J. and Hein, J. R. (1999) Osmium isotope variations in the oceans recorded by Fe–Mn crusts. *Earth Planet. Sci. Lett.* **171**, 185–197.
- Christensen, J. N., Halliday, A. N., Godfrey, L. V., Hein, J. R. and Rea, D. K. (1997) Climate and ocean dynamics and the lead isotopic records in Pacific ferromanganese crusts. *Science* **277**, 913–918.
- Gannoun, A., Burton, K. W., Parkinson, I. J., Alard, O., Schiano, P. and Thomas, L. E. (2007) The scale and origin of the osmium isotope variations in mid-ocean ridge basalts. *Earth Planet. Sci. Lett.* **259**, 541–556.
- Goto, K. T., Anbar, A. D., Gordon, G. W., Romaniello, S. J., Shimoda, G., Takaya, Y., Tokumaru, A., Nozaki, T., Suzuki, K., Machida, S., Hanyu, T. and Usui, A. (2014) Uranium isotope systematics of ferromanganese crusts in the Pacific Ocean: Implications for the marine $^{238}\text{U}/^{235}\text{U}$ isotope sys-

- tem. *Geochim. Cosmochim. Acta* **146**, 43–58.
- Graham, I. J., Carter, R. M., Ditchburn, R. G. and Zondervan, A. (2004) Chronostratigraphy of ODP 181, Site 1121 sediment core (Southwest Pacific Ocean), using $^{10}\text{Be}/^{9}\text{Be}$ dating of entrapped ferromanganese nodules. *Mar. Geol.* **205**, 227–247.
- Hassler, D. R., Peucker-Ehrenbrink, B. and Ravizza, G. E. (2000) Rapid determination of Os isotopic composition by sparging OsO_4 into a magnetic-sector ICP-MS. *Chem. Geol.* **166**, 1–14.
- Hein, J. R., Koschinsky, A., Bau, M., Manheim, F. T., Kang, J.-K. and Roberts, L. (2000) Cobalt-rich ferromanganese crusts in the Pacific. *Handbook of Marine Mineral Deposits* **18**, 239–273.
- Kato, Y., Fujinaga, K., Nakamura, K., Takaya, Y., Kitamura, K., Ohta, J., Toda, R., Nakashima, T. and Iwamori, H. (2011) Deep-sea mud in the Pacific Ocean as a potential resource for rare-earth elements. *Nature Geosci.* **4**, 535–539.
- Klemm, V., Levasseur, S., Frank, M., Hein, J. and Halliday, A. (2005) Osmium isotope stratigraphy of a marine ferromanganese crust. *Earth Planet. Sci. Lett.* **238**, 42–48.
- Klemm, V., Frank, M., Levasseur, S., Halliday, A. N. and Hein, J. R. (2008) Seawater osmium isotope evidence for a middle Miocene flood basalt event in ferromanganese crust records. *Earth Planet. Sci. Lett.* **273**, 175–183.
- Koppers, A. A. P., Staudigel, H., Pringle, M. S. and Wijbrans, J. R. (2003) Short-lived and discontinuous intraplate volcanism in the South Pacific: Hot spots or extensional volcanism? *Geochem. Geophys. Geosyst.* **4**, 1089, doi:10.1029/2003GC000533.
- Lee, D.-C., Halliday, A. N., Hein, J. R., Burton, K. W., Christensen, J. N. and Günther, D. (1999) Hafnium isotope stratigraphy of ferromanganese crusts. *Science* **285**, 1052–1054.
- Levasseur, S. (1998) Direct measurement of femtomoles of osmium and the $^{187}\text{Os}/^{186}\text{Os}$ ratio in seawater. *Science* **282**, 272–274.
- Li, J., Fang, N., Qu, W., Ding, X., Gao, L., Wu, C. and Zhang, Z. (2008) Os isotope dating and growth hiatuses of Co-rich crust from central Pacific. *Sci. China Ser. D-Earth Sci.* **51**, 1452–1459.
- Meng, X., Liu, Y., Qu, W. and Shi, X. (2008) Osmium isotope of the Co-rich crust from seamount Allison, central Pacific and its use for determination of growth hiatus and growth age. *Sci. China Ser. D-Earth Sci.* **51**, 1446–1451.
- Morgan, J. W., Golightly, D. W. and Dorrzapf, A. F., Jr. (1991) Methods for the separation of rhenium, osmium and molybdenum applicable to isotope geochemistry. *Talanta* **38**, 259–265.
- Norman, M., Bennett, V., McCulloch, M. and Kinsley, L. (2002) Osmium isotopic compositions by vapor phase sample introduction using a multi-collector ICP-MS. *J. Anal. At. Spectrom.* **17**, 1394–1397.
- Nozaki, T., Suzuki, K., Ravizza, G., Kimura, J.-I. and Chang, Q. (2012) A method for rapid determination of Re and Os isotope compositions using ID-MC-ICP-MS combined with the sparging method. *Geostand. Geoanal. Res.* **36**, 131–148.
- Paquay, F. S. and Ravizza, G. (2012) Heterogeneous seawater $^{187}\text{Os}/^{188}\text{Os}$ during the Late Pleistocene glaciations. *Earth Planet. Sci. Lett.* **349–350**, 126–138.
- Pegram, W. J. and Turekian, K. K. (1999) The osmium isotopic composition change of Cenozoic sea water as inferred from a deep-sea core corrected for meteoritic contributions. *Geochim. Cosmochim. Acta* **63**, 4053–4058.
- Pegram, W. J., Krishnaswami, S., Ravizza, G. and Turekian, K. (1992) The record of sea water $^{187}\text{Os}/^{186}\text{Os}$ variation through the Cenozoic. *Earth Planet. Sci. Lett.* **113**, 569–576.
- Peucker-Ehrenbrink, B. and Ravizza, G. (2000) The marine osmium isotope record. *Terra Nova* **12**, 205–219.
- Peucker-Ehrenbrink, B. and Ravizza, G. (2012) Osmium isotope stratigraphy. *The Geologic Time Scale 2012* (Gradstein, F. M., Ogg, J. G., Schmitz, M. and Ogg, G., eds.), 145–166, Elsevier, Amsterdam.
- Peucker-Ehrenbrink, B., Ravizza, G. and Hofmann, A. (1995) The marine $^{187}\text{Os}/^{186}\text{Os}$ record of the past 80 million years. *Earth Planet. Sci. Lett.* **130**, 155–167.
- Ravizza, G. (1993) Variations of the $^{187}\text{Os}/^{186}\text{Os}$ ratio of seawater over the past 28 million years as inferred from metalliferous carbonates. *Earth Planet. Sci. Lett.* **118**, 335–348.
- Reyss, J., Lemaître, N., Ku, T., Marchig, V., Southon, J., Nelson, D. and Vogel, J. (1985) Growth of a manganese nodule from Peru Basin: A radiochemical anatomy. *Geochim. Cosmochim. Acta* **49**, 2401–2408.
- Schoenberg, R., Nägler, T. F. and Kramers, J. D. (2000) Precise Os isotope ratio and Re–Os isotope dilution measurements down to the picogram level using multicollector inductively coupled plasma mass spectrometry. *Int. J. Mass Spectr.* **197**, 85–94.
- Shirey, S. B. and Walker, R. J. (1995) Carius tube digestion for low-blank rhenium–osmium analysis. *Anal. Chem.* **67**, 2136–2141.
- Smoliar, M. I., Walker, R. J. and Morgan, J. W. (1996) Re–Os ages of group IIA, IIIA, IVA, and IVB iron meteorites. *Science* **271**, 1099–1102.
- Usui, A., Graham, I. J., Ditchburn, R. G., Zondervan, A., Shibasaki, H. and Hishida, H. (2007) Growth history and formation environments of ferromanganese deposits on the Philippine Sea Plate, northwest Pacific Ocean. *The Island Arc* **16**, 420–430.
- Woodhouse, O. B., Ravizza, G., Kenison-Falkner, K., Statham, P. J. and Peucker-Ehrenbrink, B. (1999) Osmium in seawater: vertical profiles of concentration and isotopic composition in the eastern Pacific Ocean. *Earth Planet. Sci. Lett.* **173**, 223–233.

SUPPLEMENTARY MATERIALS

URL (<http://www.terrapub.co.jp/journals/GJ/archives/data/49/MS352.pdf>)

Figures S1 to S3

Table S1